Meron excitations in the $\nu=1$ quantum Hall bilayer and the plasma analogy

Milica V. Milovanović and Ivan Stanić
Institute of Physics, P.O. Box 68, 11080 Belgrade, Serbia and Montenegro
(Received 11 May 2005; revised manuscript received 22 August 2005; published 11 October 2005; publisher error corrected 25 October 2005)

We study meron quasiparticle excitations in the $\nu=1$ quantum Hall bilayer. Considering the well-known single meron state, we introduce its effective form, valid in the long-distance limit. That enables us to propose two (and more) meron states in the same limit. Further, establishing a plasma analogy of the (111) ground state, we find the impurities that play the role of merons and derive meron charge distributions. Using the introduced meron constructions in generalized (mixed) ground states and corresponding plasmas for arbitrary distance between the layers, we calculate the interaction between the construction implied impurities. We also find a correspondence between the impurity interactions and meron interactions. This suggests a possible explanation of the deconfinement of the merons recently observed in the experiments.

DOI: 10.1103/PhysRevB.72.155306 PACS number(s): 73.43.Cd, 73.43.Lp, 71.10.Pm

I. INTRODUCTION

The $\nu=1$ quantum Hall bilayer[1] is the subject of intensive experimental and theoretical investigations.[2] In 1995, the pseudospin theory of the bilayer[3] was advanced for this system. The theory introduced meron—a new type of quantum Hall quasiparticle. Nevertheless, even today it is not known what a construction of a pair of merons looks like.[4] Understanding of that would bring us closer to the understanding of increased susceptibility to the presence of disorder of the neutral superfluid in the pseudospin channel of the bilayer. Namely, because of the persistent dissipation in the counterflow measurments,[5,6] there is a widespread belief that even in the presence of a moderate amount of disorder, merons—vortices of the superfluid—are liberated, dissociated from one another.[2,7,8] On the other hand, since Laughlin's seminal paper,[9] the plasma analogy has proven to be a very useful concept in analyzing quasiparticle state properties.

In this paper we develop a description of the meron excitations of the pseudospin theory in the long-distance limit. We use the plasma techniques of Ref. 10, and argue that meron presence introduces a new type of impurity in the plasma analogy of the so-called (111) ground state. That enables us to easily derive meron charge distributions in the long-distance limit and infer what the construction of a pair of merons would look like in the same limit.

We also consider the same constructions in mixed, composite boson–composite fermion, ground states,[11] proposed as a way to capture in the ground state description the effect of quantum fluctuations and disordering[3] at a finite distance, d, between the layers. Charge screening of the single meron construction in the plasma analogy of mixed states is almost without change with respect to the (111) case. But the strength of the $\ln(r)$ interaction in the plasma analogy between a pair of merons gets reduced, being proportional to the density of bosons that decreases as a function of d. As detailed below, because of a formal correspondence between the interaction laws between merons and the interaction laws between impurities, this is very suggestive of a mechanism that (with composite fermion screening; see below) might be responsible for a confinement weakening. Together with disorder the mechanism may lead to the deconfinement believed to exist in the experiments.[2]

In Sec. II we discuss the plasma analogy for the (111) state, including an effective plasma description of the meron excitations above the same state. In Sec. III we deal with the plasma description of the mixed states and derive screening properties and the interaction law of the effective meron constructions above the mixed states. Section IV is devoted to discussion and conclusions.

II. (111) STATE, MERONS, AND THE PLASMA ANALOGY

In the following we will introduce plasma techniques[10] for the (111) state. Because of the unusual nature of the statistical model based on the (111) state implied by the Laughlin prescription,[9] it is not clear whether they are valid in this case, but we will show that, indeed, they can capture the leading long-distance behavior. Let us begin with the most obvious generalization of the Laughlin quasihole construction for the case of the two-component, $\uparrow$ and $\downarrow$, (111) state,

$$\Psi(w)=\prod_{i=1}(w-z_{\uparrow,i})\Psi_{111}(z_{\uparrow},z_{\downarrow}), \tag{1}$$

where the (111) state is,

$$\Psi_{111}(z_{\uparrow},z_{\downarrow})=\prod_{i<j}(z_{i,\uparrow}-z_{j,\uparrow})\prod_{k<l}(z_{k,\downarrow}-z_{l,\downarrow})\prod_{p,q}(z_{p,\uparrow}-z_{q,\downarrow}) \tag{2}$$

(with omitted Gaussian factors). To get the charge distributions at point r away from the center w of the excitation, we use an effective plasma expansion (see Ref. 10). As usual in the plasma approach,[9] we consider the exponentiated form of $|\Psi(w)|^2$, and then expand the resulting exponentials. The ensuing expansion contains the contributions that are easily visualized as a type of chain diagrams, such as shown in Fig. 1, connecting the impurity ($w=0$) to the probing point (r) on the right-hand side (rhs) Other contributions that do not in-

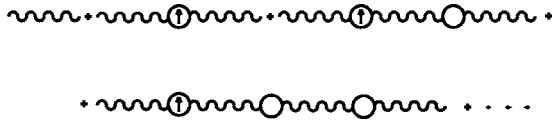

FIG. 1. Diagrammatic summation leading to the ↑ charge distribution away from an impurity.

clude both points cancel with Gaussian and other factors that represent the neutralizing background contribution. Also we do not consider in the long-distance approximation the diagrams that are simple multiples of the chain diagrams, because they can be neglected in the same approximation. Most importantly, in order to capture in the first approximation the dominant screening effects, we do not consider any other type of diagrams but chain. In Fig. 1, in the Fourier space, the wriggly line is the two-dimensional (2D) Coulomb plasma interaction, $-2\pi/|\vec{q}|^2$; the vertices are the empty circle of the value of the total density n; and the circle with up arrow denotes the density $n_\uparrow$ of the up particles. We probe the ↑ charge density at r (on the rhs in the diagrams of Fig. 1); otherwise, if we probe ↓ density, the corresponding sum does not have the first contribution in Fig. 1. Therefore, to get the ↑ and ↓ charge distributions, we have to Fourier transform ($\int d^2\vec{q}e^{i\vec{q}(\vec{w}-\vec{r})}[\cdots]$) the following expressions in which $V(\vec{q})=-2\pi/|\vec{q}|^2$,

$$\rho_\uparrow(q) = V(q) + \frac{V(q)n_\uparrow V(q)}{1-nV(q)}, \tag{3}$$

and

$$\rho_\downarrow(q) = \frac{V(q)n_\uparrow V(q)}{1-nV(q)}, \tag{4}$$

for ↑ and ↓ charge, respectively. We immediately see that the total charge is screened,

$$\rho_c(q) \sim \rho_\uparrow + \rho_\downarrow = \frac{V(q)}{1-nV(q)}, \tag{5}$$

and $\lim_{q\to 0}\rho_c(q)=$Const, like in the usual Laughlin quasihole case, but the pseudospin charge $\rho_s(q)\sim\rho_\uparrow-\rho_\downarrow=V(q)$ is unscreened, growing as $\ln(r)$ (if $w=0$) with distance r. Therefore, the capacitive energy defined as

$$E_c = \int d^2\vec{r}(\rho_\uparrow-\rho_\downarrow)^2, \tag{6}$$

which is in the first approximation proportional to the energy to excite the quasihole, is proportional to (up to logarithmic factors) the area of the system. This is the conclusion of the numerical study in Ref. 4. Therefore, the plasma analogy is able to reproduce the main result of the detailed investigation[4] (which helps us to eliminate from further consideration the constructions of the form in Eq. (1) as relevant excitations for the bilayer). The agreement does not come as a surprise if we analyze more closely the diagrams in Fig. 1. In them we are justifiably using the screening properties of the charge channel, which behaves as a plasma. Because of this, from now on, we will refer to the statistical model based on the (111) state as plasma.

In the second quantization formalism the meron excitation of the pseudospin theory[3] that parallels the construction in Eq. (1) is

$$|\Psi_m(w=0)\rangle = \prod_{m=0}^{N-1}(c^\dagger_{m+1,\uparrow}+c^\dagger_{m,\downarrow})|0\rangle. \tag{7}$$

$c^\dagger_{m,\sigma}$'s create the lowest Landau level (LLL) states, $\Phi_m=(z^m/\sqrt{2\pi 2^m m!})\exp\{-\frac{1}{4}|z|^2\}, m=0,\ldots,N-1$ (N is the number of particles in the system). In the first quantization description of Eq. (7), ↑ orbitals are shifted (in the expansion of the Slater determinant of a filled LLL) in the following manner:

$$\Phi_m(z_\uparrow) \to \frac{z_\uparrow}{\sqrt{2(m+1)}}\Phi_m(z_\uparrow). \tag{8}$$

This is a nontrivial change and cannot be described by a simple multiplication operation on the ground state, such as in Eq. (1). When $|z_\uparrow|\to\infty$, more precisely when $m=N-1\to\infty$ (i.e., m is the last orbital in the ground state), $|\Phi_m(z_\uparrow)|^2$ behaves, in the first approximation, like a delta function, at $|z_\uparrow|=\sqrt{2(m+1)}$ and, in this sense, we can approximately take for multiplying $z_\uparrow$ in Eq. (8), $z_\uparrow=\exp\{i\phi\}\sqrt{2(m+1)}$. If we extend the ansatz to lower angular momentum orbitals, except those very near the origin, the excitation looks like

$$\prod_{i=1}^{N}\begin{bmatrix}\exp\{i\phi_i\}\\ 1\end{bmatrix}\Psi_{111}(z_\uparrow,z_\downarrow) \tag{9}$$

in the first quantization.[3] To get a change in the charge distribution away from the origin we need further corrections to the limit in Eq. (9). Again we are concerned with an approximation for the last orbital, $m=N-1$, in the ground state. We do this by looking for the density distribution of the state in Eq. (7) in the first quantization [which is accompanied by the multiplication described in Eq. (8)] in which we have to approximate $|z_\uparrow|^2|\Phi_m(z_\uparrow)|^2$, $m=N-1$. The appropriate (long distance) range of $|z_\uparrow|$, for which a simple analytical approximation is expected, is beyond the delta-function peak, from $\sqrt{2(m+1)}$, to infinity. If we assume that in this range the correction is of the following form, $|z_\uparrow|^2=2(m+1)\times[1+C/|z_\uparrow|]$, we find C by solving the following equation, with $m=N-1$,

$$\begin{aligned}\int_{\sqrt{2(m+1)}}^{\infty} drr|z|^2|\Phi_m(z)|^2 &= 2(m+1)\int_{\sqrt{2(m+1)}}^{\infty} drr|\Phi_m(z)|^2 + 2(m+1)C\\ &\times\int_{\sqrt{2(m+1)}}^{\infty} dr\frac{r|\Phi_m(z)|^2}{r}.\end{aligned} \tag{10}$$

In the limit $m\to\infty$ we get $C=0.8$, as can be seen in Fig. 2. So $R=\sqrt{2(m+1)}=\sqrt{2N}$ is a characteristic shortest length for this long-range approximation, and as corrections die out as

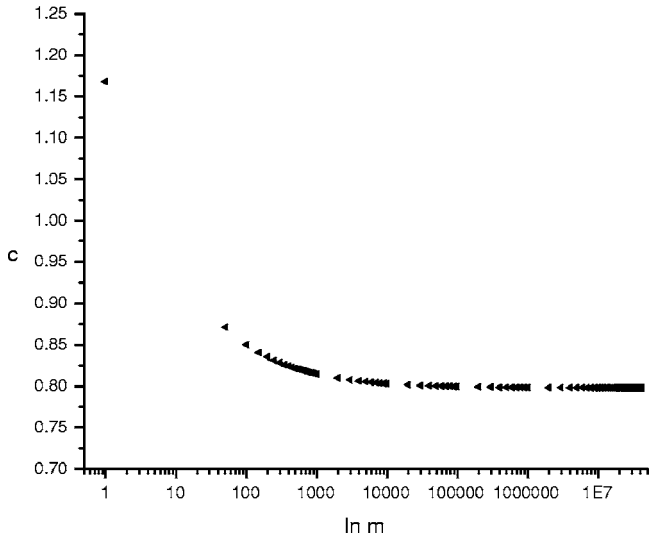

FIG. 2. Dependence of C [Eq. (10)] on $m=N-1$ (the first value at $m=1$).

$|z_\uparrow|\to\infty$ we in fact probe the physics at (and a little beyond) that length, which is a measure of the radius of the system that also grows in the thermodynamic limit. As a result we capture the longest distance physics. Therefore, in this approximation, in the approach with fixed up and down number of particles, the $\uparrow$ charge density of the excitation in Eq. (7) can be extracted from the following integral, with $|z_{\uparrow 1}|\equiv r$:

$$\rho_{w=0}(r)\sim\int d^2z_{\uparrow 2}\cdots\int d^2z_{\downarrow N}\exp\left\{\sum_i\frac{C}{|z_{i\uparrow}|}\right\}|\Psi_{111}(z_\uparrow,z_\downarrow)|^2, \tag{11}$$

and analogously for the $\downarrow$ charge density. We take that each integration has a short-distance cutoff (to avoid the singularity at the center), we have the right longest distance behavior (we simply exponentiated the $1/|z_\uparrow|$ correction so that a plasma analogy can be developed[9]), but otherwise, the rest of behavior at intermediate distances ($|z|>1$) we model as a simple continuation of the longest distance one. This choice will not influence our final conclusions because they (the density tails we want to get) depend only on the longest distance behavior in the plasma approach we take. In this way, in the (111) plasma, we consider a new type of impurity which connects via the interaction $C/(|z_{i\uparrow}|)$ to the $\uparrow$ particles of the plasma. *In this sense* we can propose the following long-distance form of the meron excitation at some point $w\neq 0$ in general,

$$\prod_i\frac{z_{i\uparrow}-w}{|z_{i\uparrow}-w|}\exp\left\{\sum\frac{C}{2|z_{i\uparrow}-w|}\right\}\cdot\Psi_{111}(z_\uparrow,z_\downarrow). \tag{12}$$

This construction can be easily generalized to the cases when there are more than one meron (of both vorticities).

To obtain the charge distributions ($\uparrow$ and $\downarrow$) far away from the center of the excitation, we use the same type of the approximation introduced in the beginning, considering Eq. (11). We get the changes in the charge distributions from the ground state values ($n_\uparrow$ and $n_\downarrow$) at some distance r from the center $w=0$ of the excitation, by Fourier transforming ($\int d^2\vec{q}e^{-i\vec{q}\vec{r}}[\cdots]$) the following expressions:

$$\rho_\uparrow(q)=V_m(q)+\frac{V_m(q)n_\uparrow V(q)}{1-nV(q)}, \tag{13}$$

and

$$\rho_\downarrow(q)=\frac{V_m(q)n_\uparrow V(q)}{1-nV(q)}, \tag{14}$$

where $V_m(q)\sim 1/q$ represents the Fourier transform of the C/r interaction. With respect to the case of the excitation in Eq. (1), we changed the way impurity connects to the plasma by switching from $V(q)\sim 1/q^2$ to $V_m(q)\sim 1/q$. In this way $\rho_\uparrow(q)\approx\frac{1}{2}V_m(q)$ and $\rho_\downarrow(q)\approx-\frac{1}{2}V_m(q)$ in the $q\to 0$ limit and for $n_\uparrow=n_\downarrow$, resulting in $E_c\sim\ln R$, where R is the radius of the system, for the energy to excite a meron, in agreement with the XY model considerations and pseudospin theory.[3]

By considering the new impurities in the (111) plasma and applying the plasma techniques, we can prove the usual XY model logarithmic interactions between them (in the plasma), which is a result without an obvious connection with the physics and the XY model of the bilayer. By considering also a pair of the old impurities [that follow from the construction in Eq. (1)], with same charge and opposite vorticity, we can find that their interaction energy in the plasma grows quadratically as a function of distance. It was found in Ref. 4, in numerics, that their real (capacitive) interaction energy behaves in the same way. Therefore the corresponding plasma have impurities with identical interaction energy laws, up to the value of couplings, to the interaction laws among corresponding quasiparticles in the quantum Hall system.

III. THE MIXED STATES, MERON EXCITATIONS, AND THE PLASMA ANALOGY

The mixed states proposed as the ground states[11] at finite (not small) d as mixtures of composite bosons of the (111) state and composite fermions of the nearby phase of two decoupled Fermi-liquidlike states can be expressed as

$$\begin{aligned}\Psi_o=\mathcal{P}\mathcal{A}\Bigg\{&\prod_{i<j}(z_{i\uparrow}-z_{j\uparrow})\prod_{k<l}(z_{k\downarrow}-z_{l\downarrow})\prod_{p,q}(z_{p\uparrow}-z_{q\downarrow})\Phi_f^\uparrow(w_\uparrow,\bar{w}_\uparrow)\\&\times\prod_{i<j}(w_{i\uparrow}-w_{j\uparrow})^2\Phi_f^\downarrow(w_\downarrow,\bar{w}_\downarrow)\prod_{k<l}(w_{k\downarrow}-w_{l\downarrow})^2\\&\times\prod_{i,j}(z_{i\uparrow}-w_{j\uparrow})\prod_{k,l}(z_{k\uparrow}-w_{l\downarrow})\\&\times\prod_{p,q}(z_{i\downarrow}-w_{q\uparrow})\prod_{m,n}(z_{m\downarrow}-w_{n\downarrow})\Bigg\}.\end{aligned} \tag{15}$$

z's and w's denote bosons and fermions respectively, $\Phi_f^\sigma,\sigma=\uparrow,\downarrow$ are two filled-Fermi-sea wave functions, $\mathcal{P}$ is the projection to LLL, and $\mathcal{A}$ is the antisymmetrizer for bosons and fermions in each layer separately. The portion of composite fermions increases as d increases. Extracting the number of flux quanta—the number of particles relations from Eq.

(15)—we can find that the number of up and down composite fermions must be the same. We have the number of flux quanta, N_Φ, is related to the number of $\uparrow$ and $\downarrow$ bosons and fermions, $N_{b\uparrow}$, $N_{b\downarrow}$, $N_{f\uparrow}$, and $N_{f\downarrow}$, respectively, as

$$\begin{aligned} N_\Phi &= N_{b\uparrow} + N_{b\downarrow} + N_{f\uparrow} + N_{f\downarrow}, \\ &= 2N_{f\uparrow} + N_{b\uparrow} + N_{b\downarrow}, \\ &= 2N_{f\downarrow} + N_{b\uparrow} + N_{b\downarrow}, \end{aligned} \tag{16}$$

leading to this conclusion. The mixed states are very close to the exact diagonalization ground states. In the following we will apply on them the weakly screening plasma approach,[10] which, again, in the long-distance approximation, was able to reproduce the basic physics of the Fermi-liquidlike composite fermion states. Because of the presence of Φ_f's, any vertex representing a connection through composite fermions is effectively the static structure factor of free Fermi gas, i.e., $s_\sigma(q) \sim q$ in the small momentum limit. Because $N_{f\uparrow}=N_{f\downarrow}$ in the mixed states, we also have $s_\uparrow = s_\downarrow$.

The expectation that the meron construction in Eq. (12) on Ψ_{111} when applied to the mixed state [Eq. (15)] comes with confinement properties similar to the ones in the (111) case can be corroborated by a calculation of the plasma interaction among the meron pair of opposite vorticity but the same charge in a mixed state. In the calculation we neglected the antisymmetrizer in Ψ_o. We state the final result,

$$\begin{aligned} V_{int}(q) = & \frac{V_m^2(q)V(q)[n_\uparrow n_\downarrow + n_\uparrow s_\uparrow(q) + n_\downarrow s_\downarrow(q)]}{1 - V(q)(n + 2s(q))} \\ & + \frac{V_m^2(q)s^2(q)}{1 - V^2(q)[2s(q)]^2} \\ & \times \left\{ nV^2(q) + \frac{n^2 + n[2s_\uparrow(q) + 2s_\downarrow(q)]}{1 - V(q)[n + 2s(q)]} V^3(q) \right\}, \end{aligned} \tag{17}$$

where $s_\uparrow(q)=s_\downarrow(q)=s(q)$ and $n_\uparrow$, $n_\downarrow$, and $n=n_\uparrow+n_\downarrow$ denote *bosonic* densities. This can be obtained straightforwardly with the help of diagrams, and the derivation can be found in Appendix A. In the $q \to 0$ limit we have,

$$V_{int}(q) \to (-)V_m^2 \frac{n_\uparrow n_\downarrow}{n} + \left(2\frac{n_\uparrow n_\downarrow}{n^2} - \frac{1}{2} \right) V_m^2(q)s(q), \tag{18}$$

i.e., the leading term is the attractive $\ln(r)$ interaction, and the correction is a $1/r$ interaction due to the screening by composite fermions that vanishes in the $n_\uparrow=n_\downarrow$ case.[12] This is a result in the formal setting of plasma analogy, but very likely, due to the mentioned correspondence, also a relevant conclusion for the interaction between two merons in the quantum Hall system. Please note again that $n_\uparrow$, $n_\downarrow$, and n are not overall densities but reduced, due to the presence of fermions, bosonic densities. Therefore, though the type of interaction $[\ln(r)]$ stays the same, the coupling strength is weaker due to its proportionality to the density of bosons.

Certainly, it is appropriate to check the amounts of the screening charges of a single meron construction in a mixed state that is the generalization of the construction in Eq. (12). Again with the help of diagrams, they can be easily found, and we will just state their limiting, $q \to 0$, behavior,

$$\rho_\uparrow(q) \to \frac{V_m(q)}{2} + \frac{n_\uparrow - n_\downarrow}{n} V_m(q), \tag{19}$$

and

$$\rho_\downarrow(q) \to \frac{V_m(q)}{2} + \frac{-2n_\downarrow}{n} V_m(q). \tag{20}$$

The complete expressions can be found in Appendix B. Therefore, in the $n_\uparrow=n_\downarrow$ case, the limits do not differ from the case without composite fermions, and we can conclude that the meron constructions in Eq. (12) applied to Ψ_{111}, when applied to the mixed state [Eq. (15)] retain their confinement property.

IV. DISCUSSION AND CONCLUSIONS

In conclusion we derived, using the plasma analogy, an effective, long-distance form of the meron excitation. That enabled us to describe the interaction law between merons for arbitrary distance between layers based on the mixed state description. From Eq. (17), the interaction law in the plasma setting, and using the expected correspondence between the laws in the plasma and real system, we can conclude, adopting the *XY* model description of the real system, that the pseudospin stiffness is propotional to the density of composite bosons. Further numerical work on the mixed state wave function[13] reveals a drastic decrease of the density of composite bosons; therefore, the pseudospin stiffness decrease with distance, especially in the experimentally available region. Thus we point out this microscopic reason, the one in the very nature of the interacting system, that together with disorder may lead to the anomalous behavior ("nonideal superfluidity"), and the presence and increased fraction of composite fermions in the mixed states in the experimental region.

The dependence of the spin stiffness on the imbalance between the layers $(n_\uparrow - n_\downarrow)$ that we can infer from Eq. (17) is consistent with existent theories of the imbalanced case (see, for example, Ref. 14), and supports our previous identification. An interesting conclusion can be drawn in that case considering Eq. (17). If the correspondence holds, the attractive interaction between merons becomes weaker in that case and the system, in the presence of disorder, is more prone to

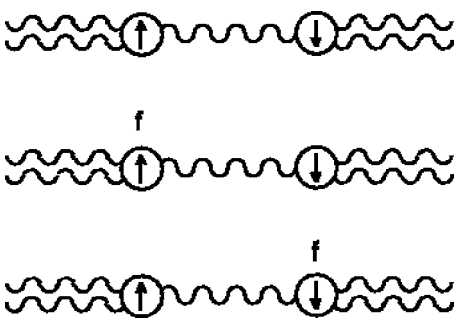

FIG. 3. Three types of connecting vertices.

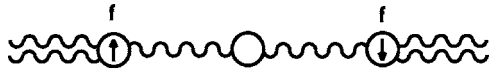

FIG. 4. The fermionic connecting vertices.

the meron deconfinement. The observed nonlinear dependence on the imbalance of the longitudinal resistances, in Refs. 15, may follow from the dependence encoded in Eq. (17), as an effect that modifies the basic (linear) behavior caused by disorder and interactions.

ACKNOWLEDGMENTS

M.V.M. thanks D. A. Huse for an inspiring conversation, N. Read, E. H. Rezayi, and S. H. Simon for previous collaborations, and Lucent Bell Labs for their hospitality during the time when this work was initiated. The work was supported by Grant No. 1899 of the Serbian Ministry of Science.

APPENDIX A

To calculate the interaction between merons of opposite vorticity, we sum chain diagrams with both bosonic and fermionic vertices and contributions. The sum has two distinct parts: one when the connecting vertices are $(n_\uparrow,n_\downarrow)$, $(s_\uparrow,n_\downarrow)$, and $(n_\uparrow,s_\downarrow)$, the first contributions are depicted in Fig. 3; and the other when they are $(s_\uparrow,s_\downarrow)$, the first contribution is depicted in Fig. 4. The double wriggly line denotes the $V_m(q)$ interaction, vertices $\uparrow$ and $\downarrow$ with a letter f (for fermionic) denote $s_\uparrow$ and $s_\downarrow$ (fermionic static structure factors), respectively, the rest of vertices denote $\uparrow$ and $\downarrow$ bosonic densities, and the vertex with an empty circle denotes the $\uparrow$ and $\downarrow$ bosonic contributions combined. The screening is obtained summing the geometric series with the increasing powers of $n_\uparrow+n_\downarrow+2s$ where $s_\uparrow=s_\downarrow=s$. It is important to notice that because $s_\uparrow=s_\downarrow=s$ the summation is possible in the form of the geometric series for this part. We depicted in Fig. 5 the first nontrivial diagram contribution for $(s_\uparrow,n_\downarrow)$, connecting vertices, which implies $n_\uparrow+n_\downarrow+2s_\uparrow$ contribution, note the doubling of the fermionic contribution because of a direct fermionic $\uparrow\uparrow$ coupling, and it is easy to see that for $(n_\uparrow,n_\downarrow)$ this is $n_\uparrow+n_\downarrow+s_\uparrow+s_\downarrow$ (Fig. 6). Due to the equivalence $s_\uparrow=s_\downarrow$ and considering the chain diagrams with arbitrary number of vertices, we come to the total contribution from this part (using the geometric series ansatz),

$$\frac{V_m^2(q)V(q)[n_\uparrow n_\downarrow + n_\uparrow s_\uparrow(q) + n_\downarrow s_\downarrow(q)]}{1-V(q)[n+2s(q)]}. \tag{A1}$$

The second part when the connecting vertices are $(s_\uparrow,s_\downarrow)$ is more involved. The first diagrams for this part are depicted

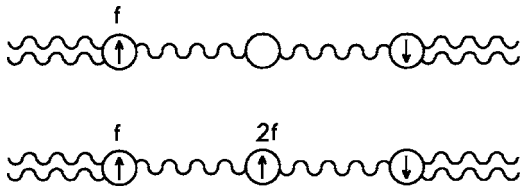

FIG. 5. The first contributions to mixed (bosonic and fermionic) connecting vertices.

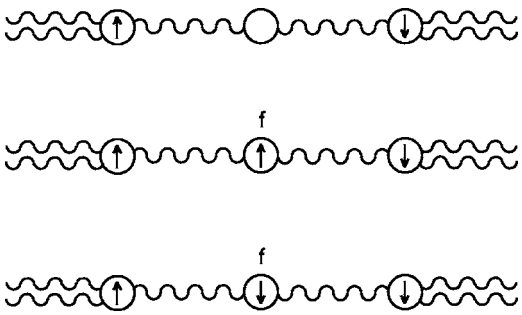

FIG. 6. The first contributions to only bosonic connecting vertices.

in Fig. 7. It is easy to recognize the existence of the screening structure where the second, third, and fourth diagrams are followed by the series and the type of screening we already had in the first part. This contributes

$$V_m^2(q)s^2(q)\left\{nV^2(q)+\frac{n^2+n[2s_\uparrow(q)+2s_\downarrow(q)]}{1-V(q)[n+2s(q)]}V^3(q)\right\}, \tag{A2}$$

but we must also recognize the intervening, additional diagrams of the type depicted in Fig. 8, which brings us to the situation similar to the beginning diagram in Fig. 7, and requires the same type of resummation. The total contribution of these additional diagrams can be put in the form of a geometric series, and therefore, in the end, the total contribution from this part is

$$\frac{V_m^2(q)s^2(q)}{1-V^2(q)[2s(q)]^2}\left\{nV^2(q)+\frac{n^2+n[2s_\uparrow(q)+2s_\downarrow(q)]}{1-V(q)[n+2s(q)]}V^3(q)\right\}. \tag{A3}$$

This combined with Eq. (A1) leads to the expression in Eq. (17).

APPENDIX B

The screening charges, $\rho_\uparrow(q)$ and $\rho_\downarrow(q)$, of a single meron construction in a mixed state can be found by regrouping of diagrams in a manner very similar to the one we already explained in Appendix A. Therefore we will just state complete, final results,

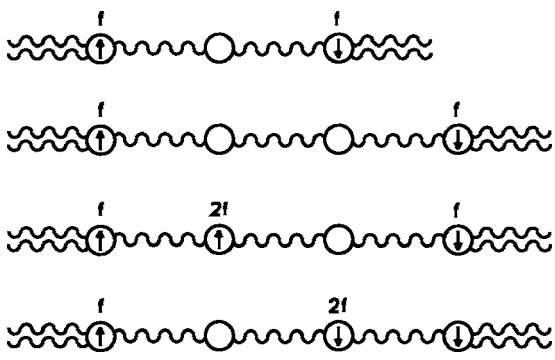

FIG. 7. The first diagrams for fermionic connecting vertices.

$$\rho_\uparrow = \frac{V_m(q)(2n_\uparrow + s_\uparrow)V(q)}{1 - V(q)[n + 2s(q)]} + V_m(q) + \frac{V_m(q)}{1 - 2s_\uparrow V(q)} + \rho^f, \tag{B1}$$

and

$$\rho_\downarrow = \frac{V_m(q)(2n_\uparrow + s_\uparrow)V(q)}{1 - V(q)[n + 2s(q)]} + \rho^f, \tag{B2}$$

where

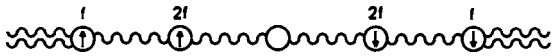

FIG. 8. An example of additional diagrams for fermionic connecting vertices.

$$\rho^f = \frac{V_m(q)s(q)}{1 - V^2(q)[2s(q)]^2} \times \left\{ nV^2(q) + \frac{n^2 + n[2s_\uparrow(q) + 2s_\downarrow(q)]}{1 - V(q)[n + 2s(q)]} V^3(q) \right\}. \tag{B3}$$

[1] For an introduction see the chapters by S. M. Girvin and A. H. MacDonald and by J. P. Eisenstein, *Perspectives in Quantum Hall Effects*, edited by A. Pinczuk and S. Das Sarma (Wiley, New York, 1997).

[2] For a more recent introduction see J. P. Eisenstein and A. H. MacDonald, Nature (London) **432**, 691 (2004).

[3] K. Moon, H. Mori, Kun Yang, S. M. Girvin, A. H. MacDonald, L. Zheng, D. Yoshioka, and Shou-Cheng Zhang, Phys. Rev. B **51**, 5138 (1995).

[4] J. Ye and G. S. Jeon, Phys. Rev. B **71**, 035348 (2005).

[5] M. Kellogg, J. P. Eisenstein, L. N. Pfeiffer, and K. W. West, Phys. Rev. Lett. **93**, 036801 (2004).

[6] E. Tutuc, M. Shayegan, and D. A. Huse, Phys. Rev. Lett. **93**, 036802 (2004).

[7] D. N. Sheng, L. Balents, and Z. Wang, Phys. Rev. Lett. **91**, 116802 (2003).

[8] D. A. Huse, cond-mat/0407452, Phys. Rev. B (to be published).

[9] R. B. Laughlin, Phys. Rev. Lett. **50**, 1395 (1983); see also R. B. Laughlin, *The Quantum Hall Effect*, 2nd ed., edited by R. E. Prange and S. M. Girvin (Springer-Verlag, New York, 1990).

[10] M. V. Milovanović and E. Shimshoni, Phys. Rev. B **59**, 10757 (1999).

[11] S. H. Simon, E. H. Rezayi, and M. V. Milovanović, Phys. Rev. Lett. **91**, 046803 (2003).

[12] Very likely this correction is not a final result because of the known difficulties of the weakly-screening plasma approach[10] in generating nonanalytic ($\sim|q|^n, n$-odd) correction to a leading behavior.

[13] G. Möller and S. H. Simon, unpublished.

[14] Y. N. Joglekar and A. H. MacDonald, Phys. Rev. B **64**, 155315 (2001).

[15] E. Tutuc and M. Shayegan, cond-mat/0504119 (unpublished); R. D. Wiersma J. G. S. Lok, S. Kraus, W. Dietsche, K. von Klitzing, D. Shoh, M. Bichler, H. P. Tranitz, and W. Weg Scheider, Phys. Rev. Lett. **93**, 266805 (2004).